

## Chapter 7

# A Biocatalytic Approach to Novel Phenolic Polymers and Their Composites

Sukanta Banerjee<sup>1</sup>, Premchandran Ramannair<sup>1</sup>, Katherine Wu<sup>1</sup>, Vijay T. John<sup>1</sup>, Gary McPherson<sup>2</sup>, Joseph A. Akkara<sup>3</sup>, and David Kaplan<sup>3</sup>

Departments of <sup>1</sup>Chemical Engineering and <sup>2</sup>Chemistry, Tulane University, New Orleans, LA 70118

<sup>3</sup>Biotechnology Division, U.S. Army Soldier Systems Command, Natick Research, Development, and Engineering Center, Natick, MA 01760-5020

We describe research to understand basic structure/function properties of conjugated phenolic polymers and their composites, and to exploit applications in enzyme delivery systems, coatings technologies and luminescent materials. The polymers are synthesized enzymatically, and the reaction is very feasible when carried out in the essentially nonaqueous system of reversed micelles. The reaction is catalyzed by horseradish peroxidase, which fully retains catalytic activity in these systems. Additionally, monomer solubility is significantly enhanced through hydrogen bonding with the surfactant. The polymer is produced in a microspherical morphology and the internal density of these microspheres can be controlled. It is possible to encapsulate enzymes in these microspheres leading to novel enzyme delivery systems. Depending on the monomer used, it is possible to prepare luminescent polymers, and polymers that bind to semiconductor nanoparticles.

The use of enzymes to synthesize novel polymers is an interesting and potentially very useful concept. There is a biomimetic aspect associated with such synthesis, the process is usually environmentally benign, and the material often has novel properties not easily achievable through chemical synthesis. We consider the synthesis of polyphenolics using an oxidative enzyme such as horseradish peroxidase, a reaction that has a mechanistic analogy in the synthesis of lignin (1). In addition to the environmentally benign aspect of synthesizing polyphenols for conventional coatings applications without the use of formaldehyde as a reaction intermediate, the enzymatic route to polyphenol synthesis leads to conjugated polymers. The feasibility of enzymatic polyphenol synthesis in organic solvents was demonstrated by Dordick et al. (2) and structural characterizations of both polyphenols and poly(aromatic amines) were done by Akkara et al. (3). The synthesis is illustrated through the simplified mechanism shown in Figure 1. Phenoxy radical centers initially formed on the monomer or growing chain migrate to the ortho positions (the para position while mechanistically allowed, is less favored) following which, coupling through condensation occurs. The direct ring-

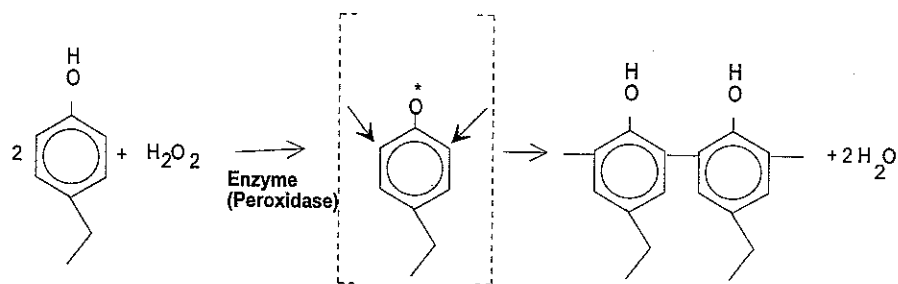


Figure 1. Simplified schematic of the polymerization reaction. The bold arrows (in the phenoxyl radical) indicate coupling in the ortho positions. The resonance structures also imply the possibility of para coupling.

to-ring coupling leads to the formation of conjugated polymers with potential applications to nonlinear optics (4).

In this paper, we review our recent research on the enzymatic synthesis of polyphenols, with a view to developing some new applications. The novelty of our method of enzymatic polymer synthesis is that we carry out the reaction in surfactant-based microstructured environments, where the system microstructure is the result of surfactant and monomer self-assembly. In particular, we have studied the environment of reversed micelles. These are water-in-oil microemulsions stabilized by surfactant. The double-tailed anionic bis(2-ethylhexyl) sodium sulfosuccinate, or AOT, shown in Figure 2a, is very effective in forming these microstructured fluid phases. Reversed micelles are capable of solubilizing macromolecules, including proteins, in the microaqueous core. Enzymes solubilized in reversed micelles are catalytically active in what is an essentially nonaqueous system. The rationale for polymer synthesis in this environment is the following. Phenolic monomers have limited solubility in water, and chain growth may be drastically retarded due to chain insolubility if the reaction is carried out in aqueous media. On the other hand, the tuning of monophasic organic solvents to maintain enzyme activity and sustain polymer growth is not always a simple task. The reversed micelle environment is an effective compromise. The enzyme is catalytically very active when solubilized in the water core, and the organic bulk phase helps support monomer and chain solubilization. A second interesting aspect of synthesis in reversed micelles is the partitioning of the polar monomer to the oil-water interface. This partitioning is the result of surfactant-phenol hydrogen bonding interactions. In dry (water-free) reversed micelles, such interactions lead to a dramatic phase transition to an organogel (5). The partitioning to the interface (depicted by the arrow of Figure 2b with the head of the arrow representing the hydroxyl moieties of the monomer) is clearly indicated by perturbations to the surfactant C=O as shown for the monomers 2-naphthol and 4-ethylphenol in Figure 3. The partitioning may result in a prealignment of the monomers before synthesis, and also provides a means of monomer replenishment to the vicinity of the enzyme. Additionally, such surfactant-monomer hydrogen bonding interactions significantly enhance monomer solubility in the reaction medium.

Polymerization in reversed micelles is very easy to carry out, and for brevity, the reader is requested to our earlier papers for details on procedures (6)(7). The self-assembling nature of the system implies that adding the enzyme dissolved in buffer (HEPES), to the surfactant and the monomer dissolved in the solvent (isooctane), leads to spontaneous formation of reversed micelles with encapsulated enzyme, and monomer partitioning to the micellar interface. Reaction is initiated through the addition of  $H_2O_2$  in small aliquots. The reaction is rapid and within 5-10 minutes of reaction initiation, over 80% of the monomer becomes converted to polymer which precipitates out of solution. An interesting aspect of the reaction conducted in reversed micelles is the observation that the polymer precipitates out in the morphology of microspheres as the scanning electron micrograph of Figure 4 illustrates. The microsphere morphology can be reproducibly obtained when the surfactant to monomer molar ratio in the micellar system is at least 3/1 (7).

This paper has a focus on two aspects of polyphenol synthesis in reversed

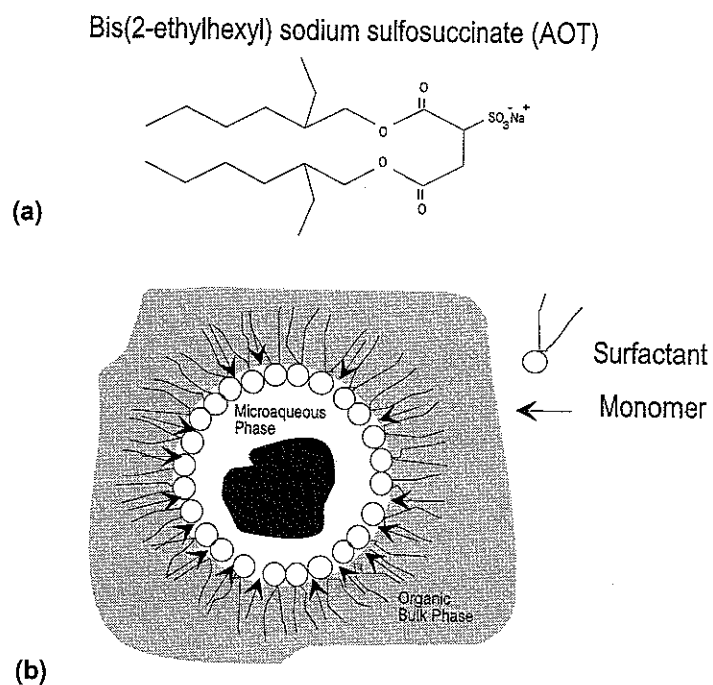


Figure 2. (a) Chemical structure of the anionic surfactant sodium bis(2-ethylhexyl) sulfosuccinate (b) Schematic of enzyme solubilized in the micelle and monomer partitioning to the micelle interface. The arrow here refers to the monomer.

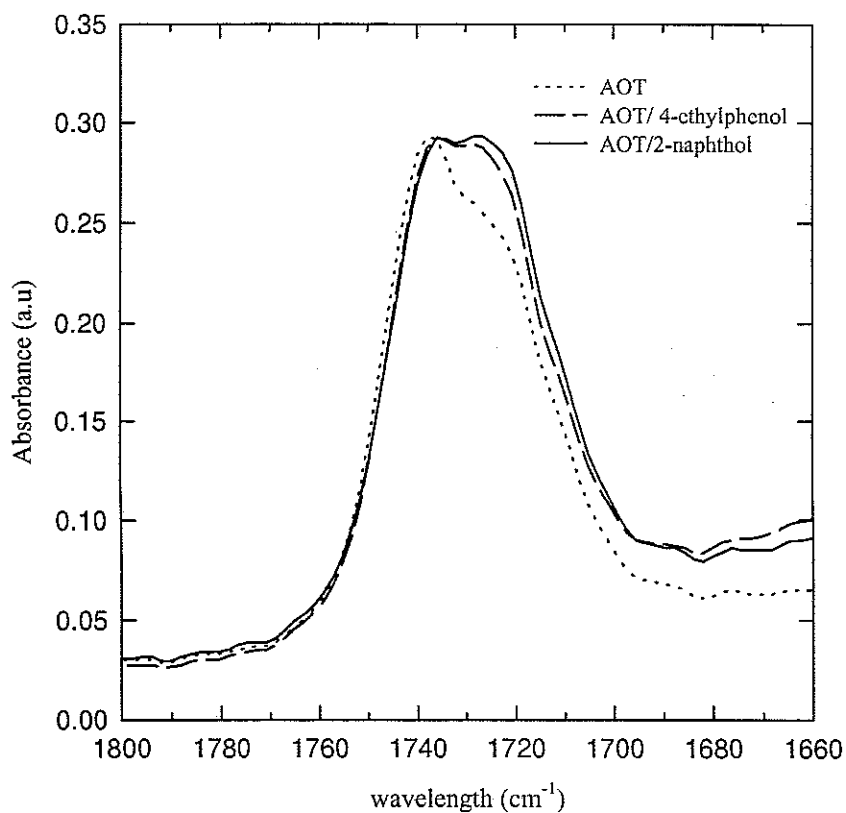
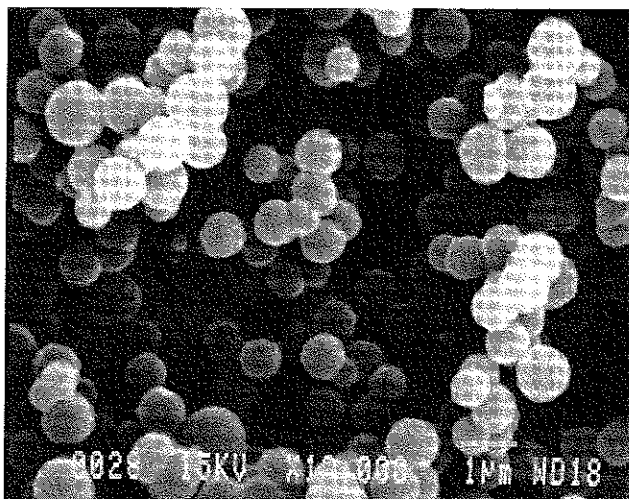


Figure 3. FTIR of the C=O stretch for the surfactant AOT. The perturbation due to hydrogen bonding with 2-naphthol is noted.



1  $\mu$ m

Figure 4. Scanning electron micrograph of poly(4-ethylphenol) prepared in the reversed micelle solution.

micelles. The first aspect is a study of the functional properties of such polymers, in particular, the concept of synthesizing fluorescent polymers and polymer-semiconductor nanocomposites. The second aspect is based on polymer morphology, where the microsphere morphology is exploited for specific applications in coatings, enzyme delivery and nanocomposite technology. The paper is essentially a summary of our recent findings with suggestions for future opportunities in this area.

### **The Enzymatic Synthesis of Functional Phenolic Polymers with Luminescent Properties**

**Polymers with Luminescent Chromophores.** Luminescent polymers have applications in technologies related to plastic scintillators, luminescent solar concentrators, high laser resistant materials, laser dyes and fiber optic sensors (8). The naphthol chromophore for example, can be used in the synthesis of polynaphthols. The enzymatic synthesis of naphthol based polymers in organic solvents has been reported (2,3) but no study has been carried out of its fluorescent properties. Poly(2-naphthol) is very efficiently synthesized in reversed micelles with polymer yields exceeding 90%. The fluorescence characteristics of the polymer are shown in Figure 5. On excitation at 327 nm (the excitation maximum for the monomer), the polymer exhibits an emission spectra with an intense peak at 375 nm and two other peaks of much lower intensity centered around 455 and 481 nm. The monomer emits at 355 nm. Thus, the band at 375 nm is assigned to emission from naphthol residues in the polymer with the 20 nm red-shift from the monomer to the polymer attributed to the increase in conjugation. However, the emission intensities at 455 nm and 481 nm get significantly stronger when the polymer is excited at 413 nm. Excitation at 413 nm reveals a well-structured and highly reproducible emission with intense peaks at 455 nm and 481 nm. These bands cannot be assigned to naphthol units and the bands represent emitting states distinct from the naphthol  $\pi$ - $\pi^*$  singlet state. Excimer/excimer based emissions are ruled out since such complexes would yield broad structureless bands independent of the excitation wavelength. Our hypothesis is that the emission at these higher wavelengths results from a more conjugated chromophore bound within the polymer. Mechanistically such chromophores can be generated through coupling at resonance positions besides the 1-1' mode. For example, 6-6' coupling followed by further oxidation to the quinonoid form shown in the inset of Figure 5 leads to a rigid, conjugated chromophore. Infrared spectroscopy points out the possible existence of quinonoid carbonyl peaks, and NMR evidence points to coupling modes besides the 1-1' positions. Further evidence comes from studies of the electrochemical oxidation of 2-naphthol indicating the possible formation of quinonoid segments (9). The rigid, planar, conjugated structure of the quinonoid segment indicates the possibility that these are the fluorophores giving rise to the emission with features at 455 and 481 nm. Since fluorescence is sensitive to trace concentrations of highly fluorescent groups in a polymer backbone when appropriately excited, it is possible that even small amounts of these fluorophores may be responsible for the structured emission at 455 and 481 nm. Figure 6 illustrates the potential of tuning fluorescence using polymers (and copolymers) from 2-naphthol and 1-hydroxypyrene. A full study of the nature of this fluorescence to

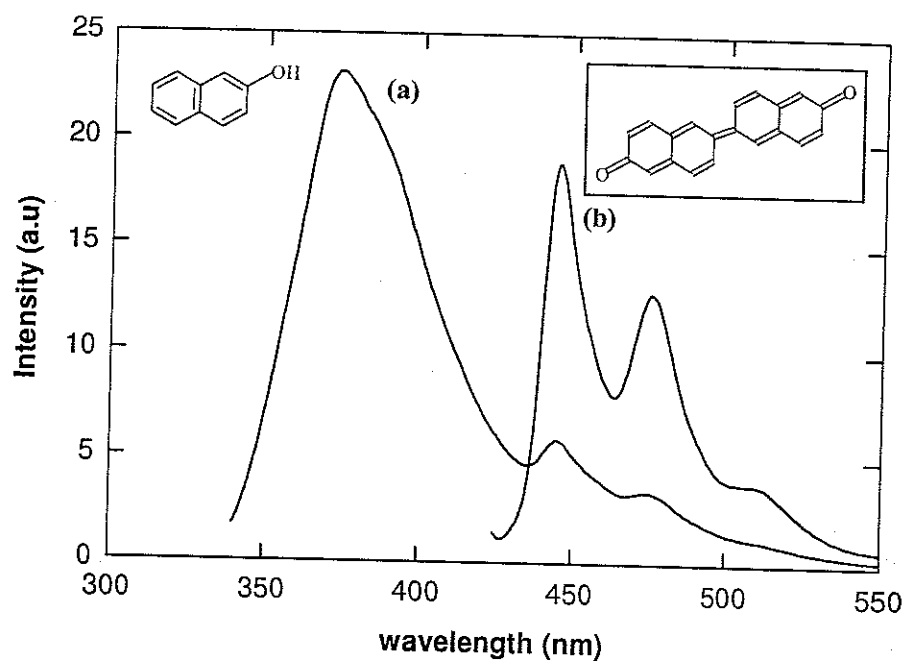


Figure 5. Fluorescence characteristics of poly(2-naphthol). Trace (a) is the emission spectrum when the polymer is excited at 327 nm, trace (b) the emission spectrum when excited at 413 nm. The second emission is tentatively attributed to the quinonoid moieties shown in the inset.

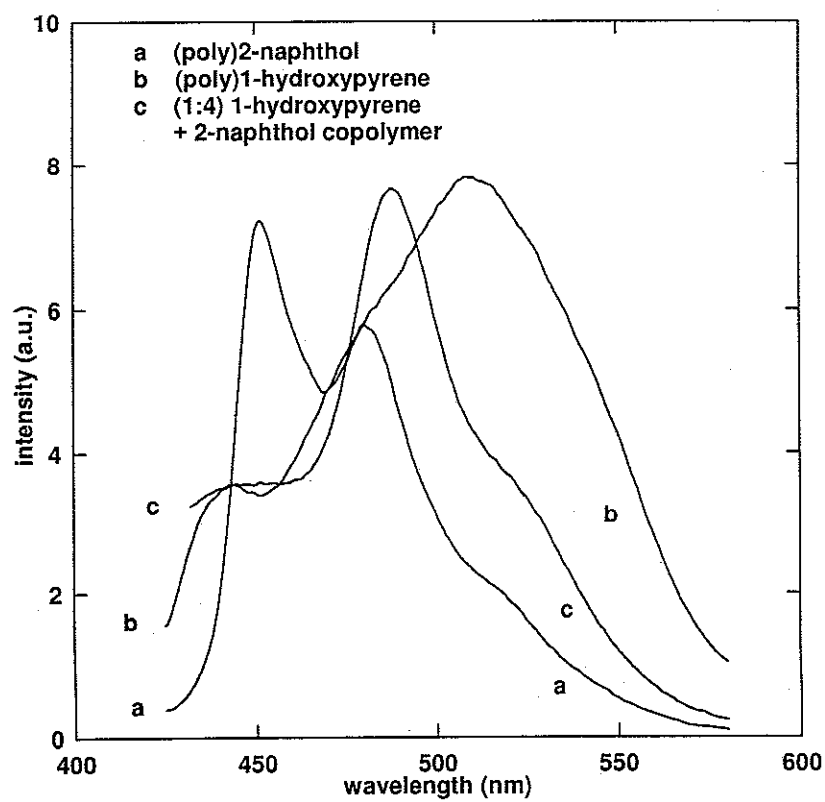


Figure 6. Fluorescence characteristics of the polymers (and a copolymer) of 2-naphthol and 1-hydroxypyrene. Excitation at 413 nm.

correlate structure to fluorescence, has not been completed. However, we note the significant Stokes shift on exciting at 413 nm, the polymer from 1-hydroxypyrene.

**Polymer-Semiconductor Nanocomposites.** A second approach to building polymers with novel optical properties is to bind semiconductor nanoparticles such as cadmium sulfide to the polymers. Such polymer-semiconductor nanocomposites possess the optoelectronic properties of the semiconductor material, and additionally may provide greater flexibility in processing. The sulfur atom of thiol compounds binds strongly to surface cadmium ions of CdS and CdSe semiconductor nanoparticles. Such surface passivation has been shown to reduce nonradiative recombinations leading to better luminescence properties (10). The objective in our work has been to use a thiol-containing monomer to prepare polymer-CdS nanocomposites. Thus, the monomer 4-hydroxythiophenol can be used for the preparation of such nanocomposites with the thiol groups on the polymer bound to CdS and CdSe nanoparticles. Again, the reversed micellar system is ideal for such synthesis. The microenvironment of the water pools restricts growth of inorganic clusters to the nanometer size range. Nanoparticle size can be controlled simply by adjusting micelle size, which in turn is directly related to the system water content (11) (the quantity,  $w_0$ , the water to AOT molar ratio is a measure of micelle size). The micellar environment allows CdS to be synthesized with bandgap values varying from the bulk material (2.4 eV) up to about 3 eV with particle sizes approaching 2 nm (12).

Although both CdS and 4-hydroxythiophenol containing polymers can be synthesized in reversed micelles, there are some nuances to the procedure. First, since  $\text{Cd}^{2+}$  rapidly deactivates HRP, the CdS synthesis has to be done separately from the enzymatic polymer synthesis. The procedure that we have adopted is to first synthesize 4-hydroxythiophenol containing polymers and then contact the polymer with CdS nanoparticles. When reaction in reversed micelles is carried out with pure 4-hydroxythiophenol, the product is an insoluble precipitate that is hard to process. This is probably due to  $\text{H}_2\text{O}_2$  induced oxidation of thiol groups leading to the formation of disulfide bonds, which gives rise to a highly crosslinked, unprocessable material. However, copolymers of 4-hydroxythiophenol and 4-ethylphenol are very easy to synthesize, and the product shows retention of thiol groups (FTIR analysis). After synthesis, the copolymer is dissolved in dimethylsulfoxide and saturated with CdS nanoparticles. Figure 7 illustrates fluorescence characteristics of these copolymers. It is seen that as the fraction of 4-hydroxythiophenol in the copolymer increases, the fluorescence intensity increases indicating a greater saturation of CdS in the polymer. Atomic absorption analysis of polymer cadmium content indicates an increase from 3 wt% cadmium in copoly(10% 4-hydroxythiophenol, 90% 4-ethylphenol) to 7.2 wt% cadmium in copoly(50% 4-hydroxythiophenol, 50% 4-ethylphenol). An interesting aspect of the fluorescence is that nanoparticle capping by the polymer significantly cuts off low energy surface recombinations (which usually show up around 540 nm); the emission observed corresponds to recombinations with near bandgap energies. The polymer-capped CdS nanocomposite is remarkably stable in solution as opposed to colloidal CdS which precipitates out due to Ostwald ripening and photocorrodes upon exposure to light and oxygen (13). We note that up to about 60% 4-hydroxythiophenol

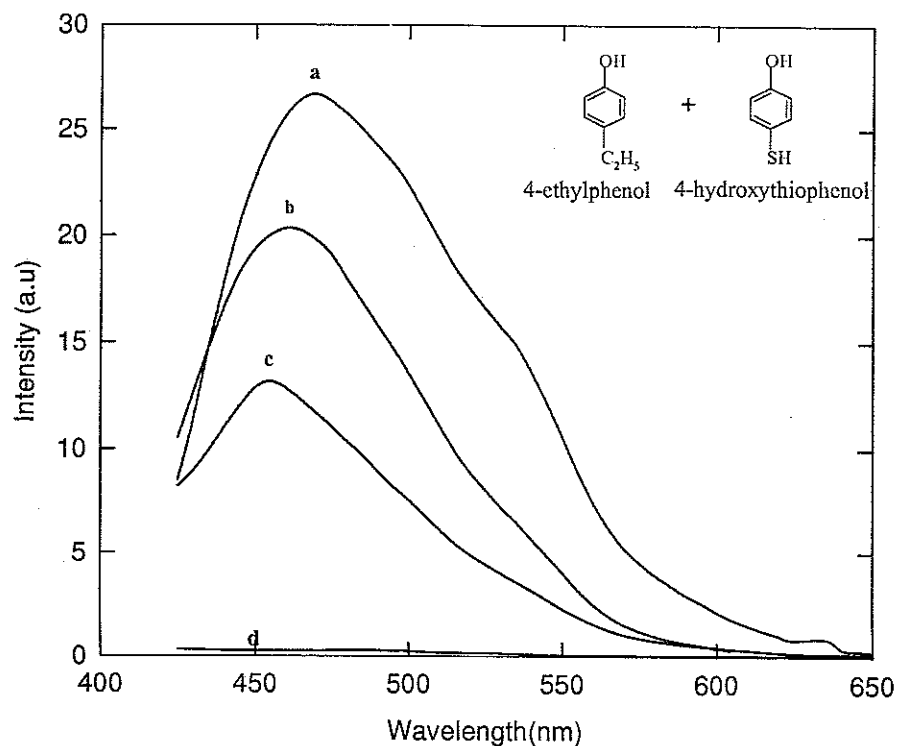


Figure 7. Fluorescence characteristics of polyphenol-CdS composites. The monomer ratios used to make the of the various copolymers (a) 1/1 4-ethylphenol (EP)/ 4-hydroxythiophenol (HTP), (b) 7/3 EP/HTP, (c) 9/1 EP/HTP. Curve (d) is the polymer of (b) but without CdS. As the HTP content increases, the amount of CdS bound to the polymer also increases as shown by the intensity enhancement.

in the monomer mixture, the copolymer precipitates out from reversed micelles in the microsphere morphology of Figure 3, and can be easily dissolved in a number of polar solvents. At higher levels of the 4-hydroxythiophenol component, the morphology is lost and the precipitate becomes unprocessable, perhaps due to the prevalence of disulfide bonds.

### Applications resulting from polymer morphology

Two important aspects result from the the observation that the enzymatic route to polyphenol synthesis in reversed micelles leads to polymers with the morphology of microspheres.

1. The internal density of the microspheres can be controlled by adjustment of reaction time and  $H_2O_2$  addition (14). This is so because the microspheres contain enzyme and unreacted monomer, and polymerization continues even after the overall morphology has been achieved, leading to densification. Figure 8 illustrates the densification of the microspheres as observed through transmission electron microscopy. The diffuse microspheres of Figure 8a form within 5-15 minutes of reaction initiation, while continuing reaction over 24 hours results in the dense microspheres of Figure 8b. By stopping reaction after the first 15 minutes and washing the polymer to remove residual monomer and  $H_2O_2$ , it is possible to arrest densification.
2. During precipitation, the polymer also encapsulates solutes located in the water core of the micelle. This may be a novel method, perhaps a ship-in-a-bottle approach to microencapsulation. The solutes include both organic water-soluble macromolecules such as proteins, and inorganic nanoclusters.

Let us consider two examples of such microencapsulation. In the first example, ferrite nanoparticles are synthesized in the micellar environment with a size of the order of magnetic domain size. The particles then have room temperature superparamagnetic properties. After particle synthesis, monomer and enzyme are added to the micellar system and polymerization conducted. The interfacial nature of polymerization results in an encapsulation of the ferrite particles in the polymer chains, the final polymer precipitates contain ferrite nanoparticles. Figure 9 illustrates a cut-section TEM of a single polymer particles with the dark spots being ferrite nanoparticles. These composites exhibit superparamagnetism (15) and being in the form of microspheres can be easily dispersed for magnetic coatings applications. Additional applications include the use of these composites for magnetic bioseparations since phenolic materials can be easily functionalized to bind to specific antibodies (16). The use of these magnetic microspheres as contrast agents in magnetic resonance imaging is another potential application.

The second example is on enzyme encapsulation. Here, other enzymes are cosolublized with HRP in the reversed micelle system. When polymerization is carried out, the precipitating polymer not only traps HRP but also the cosolublized enzyme. Short duration polymerization to maintain the diffuse internal density of the microspheres, results in polymer-enzyme composites that retain the catalytic activity of the entrapped enzyme (accommodating for diffusional limitations). For example, we have shown that phosphodiesterase entrapped in the microspheres is catalytically active and has an enhanced stability compared to the free enzyme (13).

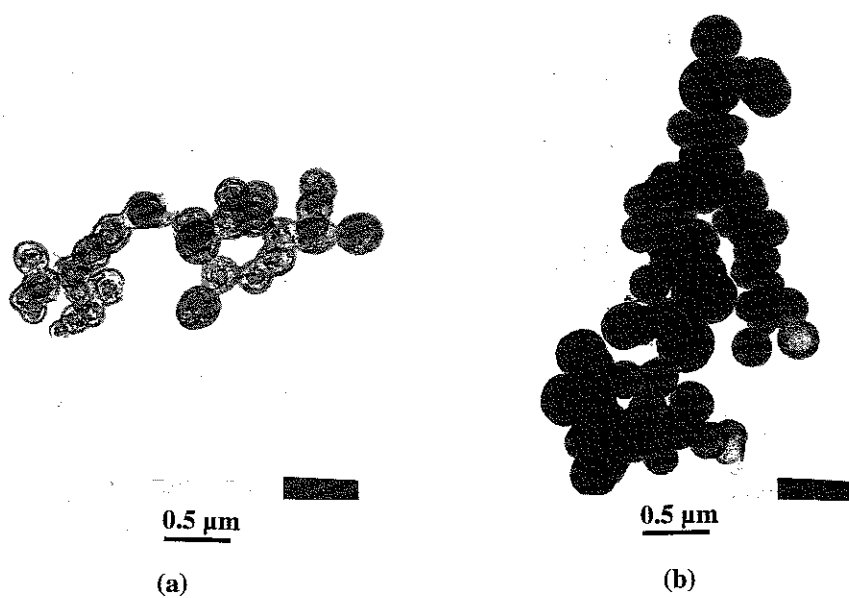


Figure 8. Transmission electron micrographs of (a) diffuse microspheres (after 15 mins reaction) and (b) dense microspheres (after 24 hours reaction).

However, activity retention is also dependent on the ability of the enzyme to survive the oxidative addition of  $H_2O_2$  to initiate polymerization. Metalloenzymes may not always be good candidates for microencapsulation through this method, due to some  $H_2O_2$  induced deactivation. To circumvent the problem, we have carried out a two step process of metalloenzyme microencapsulation (17). The phenolic polymer is first synthesized in reversed micelles using HRP. Subsequently the polymer is dissolved at high concentrations in a solvent (acetone, or benzene). The polymer solution is then contacted with a much larger volume of a reversed micellar solution containing the enzyme of interest. Since the reversed micellar solution is a nonsolvent, the polymer reprecipitates. Interestingly the precipitate has a microsphere morphology. As a possible consequence of surfactant-polymer interactions, we find that the enzyme cosolubilized in the micelles is again entrapped in the polymer microspheres with high efficiency (16). Figure 10 illustrates an interesting hollow microsphere morphology upon polymer precipitation in the micellar nonsolvents. In recent research, we have encapsulated the phosphotriestase from *Pseudomonas diminuta* into these microspheres. The enzyme is capable of hydrolyzing organophosphorus compounds including nerve agents (18). While the free enzyme has a turnover frequency of about  $3000\text{ s}^{-1}$  ( $k_{cat}$  values) for the hydrolysis of paraoxon, we have been able to approach values of  $500\text{ s}^{-1}$  with the encapsulated enzyme. The Lineweaver-Burk plot of Figure 11 reports the Michaelis-Menten parameters for the hydrolysis of paraoxon. The lyophilized polymer-enzyme composite has good shelf life. The results indicate the viability of the composite in technologies related to chemical decontamination. The catalytic microspheres may be used to make protective coatings on fabrics. Or they may be sprayed onto the site of chemical decontamination. As a result of encapsulation, the enzyme may be protected from shear-induced denaturation upon spraying. Studies are in progress to test the efficacy of the composite after being subjected to shear, and in the presence of foams.

### Summary and Future Directions

The results described indicate the potential of using enzymes to couple phenols to produce functionally useful polymers, with particular emphasis on polymers and polymer-semiconductor composites with luminescent properties. The possibility of deriving fluorescence either from the polymeric component or from the semiconductor nanoparticle adds considerable flexibility to the synthesis scheme. The fact that these are conjugated polymers implies the possibility of electroluminescence. These materials may therefore represent a new class of polymeric electronic materials, and polymeric photocatalysts, with electronically coupled quantum dot clusters (19). Continuing studies seek to clarify these issues and to delineate new applications. Dual application possibilities also exist with enzymatically coupled dihydroxynaphthalenes. The recent, remarkable report by Dordick and coworkers (20) indicates an indirect approach to poly(hydroquinone) synthesis using a multienzyme, chemoenzymatic method to avoid direct peroxidase-catalyzed oxidation of hydroquinone to benzoquinones. The resulting polymer is redox active and has many electrochemical applications in battery and sensor technologies. Polymers from 2,6-dihydroxynaphthalene may have both redox activity and fluorescence properties, widening their applications to chemical sensors.

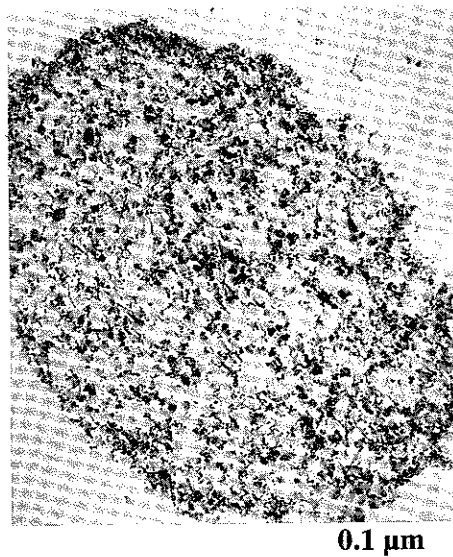


Figure 9. A cut section transmission electron micrograph of ferrite nanoparticles embedded in polyphenol microspheres. The elliptical cross-section is due to distortion during sectioning.

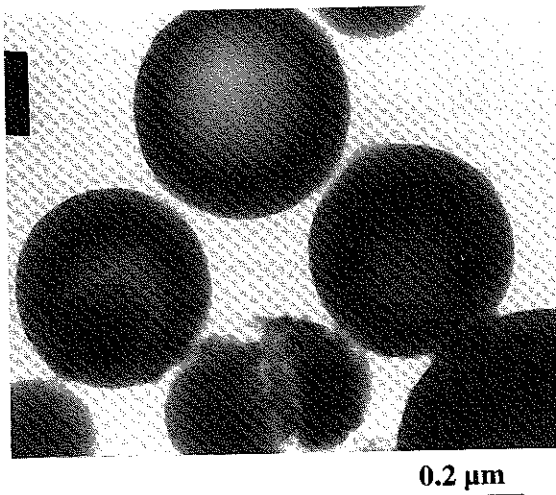


Figure 10. Polymer precipitation using a micellar nonsolvent. The TEM indicates partially hollow microspheres formed as a result of phase segregation between incorporated water in the microsphere and the bulk organic phase.

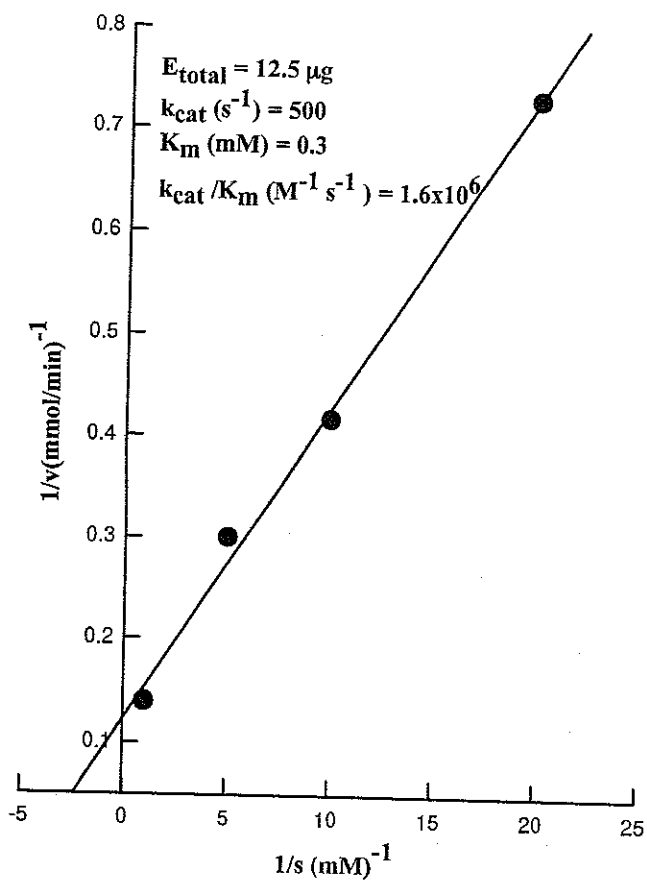


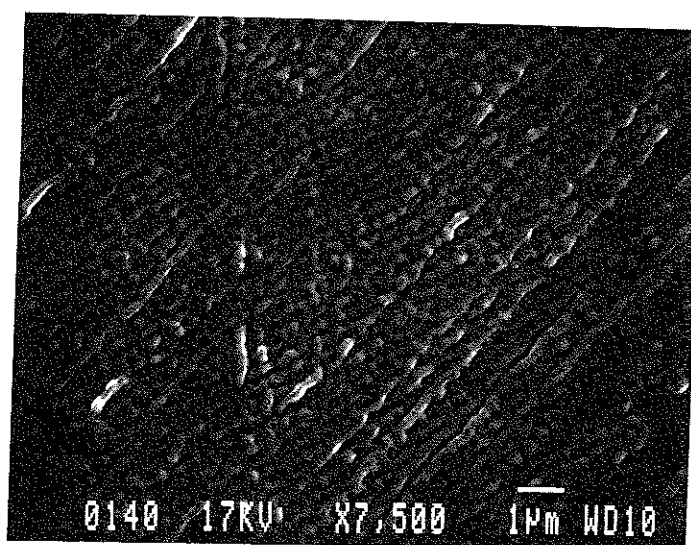
Figure 11. Lineweaver-Burk plot of phosphotriesterase activity when encapsulated in polymer microspheres. The reaction is the hydrolysis of paraoxon (diethyl *p*-nitrophenylphosphate). Nitrophenol formation is monitored by absorbance at 410 nm.

The nature of synthesis in reversed micelles and surfactant microstructures provides another interesting aspect meriting further study. We have shown that the reversed micellar environment influences polymer formation in the morphology of microspheres whose internal density can be controlled. The mechanism of particle formation and polymer precipitation also involves encapsulation of intramicellar solutes. Polyphenol precipitation in a micellar nonsolvent is an alternate method of microencapsulation. Our results have shown the potential for preparing polymeric microspheres containing active enzymes, or inorganic materials. An extension would be the development of polymer-polymer composites where polyphenols are folded around other polymeric nanoparticles synthesized in reversed micelles.

Finally, the remarkable nature of the enzymatic polymer synthesis in microstructured environments is demonstrated through some very recent results illustrated in the SEM of Figure 12. Here we synthesize poly(4-ethylphenol) in a hard, clear gel made with lecithin (phosphatidylcholine), AOT, water and isooctane. The species concentrations are 0.2M (lecithin), 0.4 M (AOT) and  $w_0$  ( $[H_2O]/[AOT]$ ) = 70. The composition of the gel is such that the water and isooctane volumes used are almost equivalent, so that the gel is neither an aqueous gel nor an organogel. The gel is formed by repeated warming and cooling and the formation occurs over a period of a few hours. The gel is an extension of the lecithin organogels formed by Luisi and coworkers (21) with the difference being the inclusion of AOT as an additional component, and a much larger water content. We have found that the gels are also formed easily in crude lecithin preparations (Sigma Type IV-S, from soybean, for example) which are much less expensive than purified lecithin. The objective of doing polymerization in these gels was to conduct the reaction in a medium which would prevent phase separation of the polymer from the monomer, and thereby allow continued growth. The aqueous gel microphase is used to sustain the enzyme, while the organic gel microphase helps solubilize the monomer. As polymerization proceeds, the polymer can be visually observed growing throughout the gel phase (as a deep grey color spreading through the medium). The polymer formed in this environment was imaged by simply dipping a microscope stub (face-down) into the gel, followed by gentle washing with isooctane to remove the adsorbed AOT and lecithin. As Figure 12 indicates, there is a furrow-like pattern to the polymer. The furrows appear to be made up of coalesced microspheres. It is unclear whether this pattern formation is the result of interfacial polymerization, or of polymerization in the restricted geometry of the organic phase which sustains the monomer. Nevertheless, the results indicate new and fascinating approaches to polymer templating. It may be possible to grow inorganic materials in the channels between the polymer strings, leading to the formation of new composites. There are many such aspects of polymer and composite synthesis in surfactant based microstructures that deserve further study.

#### Acknowledgement

Financial support by the U.S. Army, the National Science Foundation, and the Tulane/DoD Center for Bioenvironmental Research is gratefully acknowledged. We are grateful to Dr. Frank Raushel (Texas A&M University) for a sample of phosphotriesterase from *Pseudomonas diminuta*.



1 µm

Figure 12. Polymer morphology and arrangement when synthesized in lecithin + AOT gels.

### Safety Considerations

Cadmium compounds and hydroxythiophenol are toxic and should be handled with appropriate precautions. The MSDS sheets on all organic compounds should be consulted before use.

### References

1. B. Halliwell and J.M.C. Gutteridge, *Free Radicals in Biology and Medicine*, Clarendon Press, Oxford, 1989.
2. Dordick, J.; Marletta, M.A.; Klibanov, A.M. *Biotechnol. Bioeng.* **1987**, *30*, 31.
3. Akkara, J.A.; Senecal, K.J.; Kaplan, D.L. *J. Polym. Sci.* **1991**, *29*, 1561.
4. Akkara, J.A.; Ayyagari, M.; Bruno, F.; Samuelson, L.; John, V.T.; Karayigitoglu, C.; Tripathy, S.; Marx, K.A.; Rao, D.V.G.L.N.; Kaplan, D.L. *Biomimetics* **1994**, *2*, 331.
5. Tata, M.; John, V.T.; Waguespack, Y.Y.; McPherson, G.L. *J. Phys. Chem.* **1994**, *98*, 3809.
6. Rao, A.M.; John, V.T.; Gonzalez, R.D.; Akkara, J.A.; Kaplan, D.L. *Biotechnol. Bioeng.* **1993**, *41*, 531.
7. Karayigitoglu, C.; Kommareddi, N.; John, V.; McPherson, G.; Akkara, J.; Kaplan, D. *Materials Science and Engineering. C: Biomimetic Materials, Sensors and Systems* **1995**, *2*, 165.
8. Barashkov, N.N.; Gunder, O.A. *Fluorescent Polymers*, Ellis Horwood Series in Polymer Science and Technology: New York, **1994**.
9. Pham, P.C.; Lacaze, P.C.; Genoud, F.; Dao, L.H.; Nguyen, M. *J. Electrochem. Soc.* **1993**, *140*, 912.
10. Majetich, S.A.; Carter, A.C. *J. Phys. Chem.* **1993**, *97*, 8727.
11. Pileni, M.P.; Zemb, T.; Petit, C. *Chem. Phys. Lett.* **1985**, *118*, 4.
12. Henglein, A. *Chem. Rev.* **1989**, *89*, 1861.
13. Robinson, B.H.; Towey, T.F.; Zourab, S.; Visser, A.J.W.B.; van Hoek, A. *Colloids Surf.* **1991**, *61*, 175.
14. Xu, X.; Kommareddi, N.; McCormick, M.; Baumgartner, T.; John, V.T.; McPherson, G.L.; Akkara, J. A.; Kaplan, D.L.; *Materials Science and Engineering C: Biomimetic Materials, Sensors and Systems* **1996**, *4*, 161.
15. Kommareddi, N.S.; Tata, M.; John, V.T.; McPherson, G.L.; Herman, M.; Lee, Y.S.; O'Connor, C.J.; Akkara, J.A.; Kaplan, D.L. *Chemistry of Materials*, **1996**, *8*, 801.
16. Nustad, K.; Danielson, H.; Rieth, A.; Funderud, S.; Lea, T.; Vartdal, F.; Ugelstad, J. In *Microspheres: Medical and Biological Applications*, Rembaum, A., Tokes, Z.A., Eds.: CRC Press: Boca Raton, FL, 1988: p 53.
17. Banerjee, S.; Premchandran, R.; Tata, M.; John, V.; McPherson, G.; Akkara, J.; Kaplan, D. *Ind. Eng. Chem. Research* **1996**, *35*, 3100.
18. Dumas, D.P.; Caldwell, R.; Wild, J.R.; Raushel, F.M. *J. Biol. Chem.* **1989**, *264*, 19659.
19. Noglik, H.; Pietro, W.J. *Chem. Mater.*, **1995**, *7*, 1333.
20. Wang, N.; Martin, B.D.; Parida, S.; Rethwisch, D.G.; Dordick, J.S. *J. Amer. Chem. Soc.*, **1995**, *117*, 12885.
21. Capitani, D.; Rossi, E.; Segre, A.L.; Giustini, M.; Luisi, P.L. *Langmuir*, **1993**, *9*, 685.